Med Chem Res (2014) 23:1512–1518
DOI 10.1007/s00044-013-0763-5

MEDICINAL CHEMISTRY RESEARCH

ORIGINAL RESEARCH

Hologram quantative structure–activity relationship studies on 1-(5-carboxyindol-1-yl)propan-2-one inhibitors of human cytosolic phospholipase $A_2\alpha$

Xiang-Lin Yang · Yuan Zhou · Xin-Ling Liu

Received: 1 May 2013 / Accepted: 23 August 2013 / Published online: 1 September 2013

Abstract A series of structurally related indole-5-carboxylic acids as potent inhibitors against human cytosolic phospholipase $A_2\alpha$ ($cPLA_2\alpha$) were subjected to hologram quantative structure–activity relationship (HQSAR) analysis. A training set containing 23 compounds served to establish the HQSAR model. The best HQSAR model was generated using atoms, bond, connectivity, donor and acceptor as fragment distinction, and 3–6 as fragment size with five components showing cross-validated q^2 value of 0.790 and conventional r^2 value of 0.961. The model was then employed to predict the potency of five test set compounds that were excluded in the training set, and a good agreement between the experimental and predicted values was observed exhibiting the powerful predictable capability of this model ($r^2_{pred} = 0.605$). Contribution maps indicated that the carboxylic acid moiety in position 5 of the indole scaffold and the electron-withdrawing effects contributed to the inhibitory activity. Based upon some key structural features derived from HQSAR 2D contribution maps, we have designed novel inhibitors of $cPLA_2\alpha$ possessing better inhibitory activity.

Keywords $cPLA_2\alpha$ inhibitors · HQSAR · Fragment size · Hologram length

X.-L. Yang
College of Chemistry and Chemical Engineering, Hunan University of Science and Technology, Xiangtan 411201, Hunan, China

Y. Zhou (✉) · X.-L. Liu
College of Chemistry and Chemical Engineering, Hunan Institute of Engineering, Xiangtan 411104, Hunan, China
e-mail: zhouyuanzy@126.com

Introduction

Cytosolic phospholipase $A_2\alpha$ ($cPLA_2\alpha$) is an esterase that selectively catalyzes the hydrolysis of the sn-2 ester of arachidonate-containing membrane phospholipids to generate free arachidonic acid and lysophospholipids (Ghosh *et al*., 2006; Kita *et al*., 2006). The freed arachidonic acid is rapidly oxidized via cyclooxygenase (COX) and lipoxygenase (LO) pathways to eicosanoids such as prostaglandins, which play a major part in the inflammatory response, and leukotrienes, which play a main role in the pathogenesis of asthma. Remaining lysophospholipids with an alkyl ether moiety at the sn-1 position can be acetylated to platelet-activating factor (PAF), another mediator of inflammation. Although several other phospholipases A2 are present in the mammalian organism, the predominance of $cPLA_2\alpha$ for lipid mediator generation was demonstrated especially by studies with $cPLA_2\alpha$-deficient mice (Bonventre *et al*., 1997; Hegen *et al*., 2003; Miyaura *et al*., 2003; Nagase *et al*., 2000; Sapirstein and Bonventre, 2000; Uozumi *et al*., 1997). These animals, which show a reduced eicosanoid production, are immune to disease in a variety of models of inflammation, including collagen-induced arthritis. Therefore, this enzyme ($cPLA_2\alpha$) can be regarded as a target for inflammatory diseases (Bonventre, 2004).

Despite the fact that there have been intense efforts for developing inhibitors of $cPLA_2\alpha$ (Clark and Tam, 2004; Connolly and Robinson, 1995; Lehr, 2006; Magrioti and Kokotos, 2010), only a few substances with high in vitro potency have been found so far, such as the thiazolidinedione (Seno *et al*., 2000, 2001), the benzhydrylindole (efipladib) (Lehr, 2006; Lee *et al*., 2007, 2008; McKew *et al*., 2008), and the 1,3-diaryloxypropan-2-one (AR-C70484XX) (Chen *et al*., 2009). A common deficiency of

these inhibitors is their high lipophilicity, which leads to low aqueous solubility and as a result of this to poor bioavailability. For this reason, efforts have been started to reduce the lipophilicity of such cPLA$_2\alpha$ inhibitors. Recently, a series of structurally related indole-5-carboxylic acids with low lipophilicity were reported to be potent inhibitors of human cPLA$_2\alpha$ (Drews *et al*., 2010). Structure–activity relationship studies on these inhibitors were investigated by the modification of the electrophilic ketone group in the middle part of the molecule, only to find that all derivatives were less active than the lead compound (Kaptur *et al*., 2011). A 3D-QSAR pharmacophore model consisting of hydrogen bond acceptors, negative, and aromatic rings was developed, giving some ideas about possible interactions (Jain *et al*., 2013). However, these SAR and quantative structure–activity relationship (QSAR) studies failed to synthesize or design more potent cPLA$_2\alpha$ inhibitors based on the 1-(5-carboxyindol-1-yl)propan-2-one scaffold. The necessity of developing more potent QSARs with good predictive insight into the structure requirement for cPLA$_2\alpha$-binding affinity is urgently needed, which can facilitate the discovery of cPLA$_2\alpha$ inhibitors with improved biological activity. Due to its effectiveness, fastness, and high predictive power, holographic QSAR is becoming increasingly an important drug design tool that encodes fragment-based information of molecular structures. Therefore, as part of this research program aimed at discovering more potent cPLA$_2\alpha$ inhibitors with appropriate lipophilicity, we have employed the hologram QSAR (HQSAR) method to generate predictive 2D QSAR models, which has rarely been reported before. On the basis of the established HQSAR model, we attempted to elucidate a structure–activity relationship to provide useful guidelines for the design of more potent cPLA$_2\alpha$ inhibitors.

Experiment and computation

Datasets and molecular modeling

In vitro inhibitory activity of the 1-(5-carboxyindol-1-yl)propan-2-one inhibitors of human cPLA$_2\alpha$, which has been reported (Drews *et al*., 2010), was taken for the study (Table 1). The biological data taken from the literature as IC_{50} value of cPLA$_2\alpha$ inhibition was converted to the corresponding pIC_{50} ($-\log IC_{50}$) and used as dependent variables in HQSAR analysis. The pIC_{50} values span a range of 3 log units, providing a broad and homogenous dataset for the HQSAR study. Taking the structural diversities and wide range of activity into account, the compounds were divided randomly into training and test set. Meanwhile, a little care was taken in the selection of test sets, so that representatives of all compounds were included for prediction. 23 out of total 28 compounds were included in the training set to derive the HQSAR model while the remaining five were used as test set to validate the external predictability of model. Molecular modeling studies were performed using the SYBYL 8.1.1 software package (Tripos, L.P., St. Louis, MO, USA) running on a HP Z600 workstation.

HQSAR analysis

HQSAR is a modern QSAR technique developed from unity hashed fingerprint concept, which employs specialized fragment fingerprints as predictive variables of biological activity (Heritage Trevor and Lowis David, 1999). Compared with other existing QSAR methods, HQSAR not only avoids the need for 3D structure, putative binding conformations, and molecular alignment in CoMFA (Cramer *et al*., 1988) and CoMSIA (Klebe *et al*., 1994), but also averts the selection and calculation or measurement of the physicochemical descriptors required by classical QSAR. HQSAR analysis involves three main steps: the generation of substructural fragments for each of the molecules in the training set; the encoding of these fragments in holograms; and correlation of the latter with the available biological data.

In HQSAR, the input molecule is broken into a series of unique structural fragments (linear, branched, and overlapping) containing user-defined minimum and maximum number of atoms. According to a predefined set of rules that encodes the frequency of occurrence of various molecular fragment types, the hashed fingerprint is obtained. Then, this hashed fingerprint is divided into strings at a fixed interval as determined by a hologram length (HL) parameter. The strings are then aligned and the sum of each column constitutes the individual component of the molecular hologram of a particular length.

A number of parameters concerning hologram generation, such as HL, fragment size, and fragment distinction, prevailingly affect the HQSAR model quality (Heritage Trevor and Lowis David, 1999). In order to derive the best HQSAR model, it is necessary to discuss the influence of various combinations of parameters on the HQSAR model. All models generated in these studies were evaluated using full cross-validated q^2, partial least squares (PLS), and leave-one-out (LOO) method.

Predictive correlation coefficient (r^2_{pred})

The predictive ability of the HQSAR models was expressed with predictive correlation coefficient (r^2_{pred}), defined as:

$$r^2_{pred} = (SD - PRESS)/SD$$

where SD is the sum of squared deviations between the biological activity of the test set and the mean activity of

Table 1 Chemical structures, experimental and predicted activities, and residuals of compounds included in the training set and test set

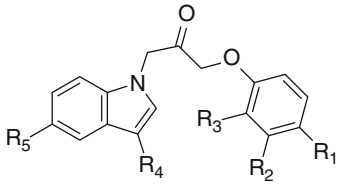

Compound	R_1	R_2	R_3	R_4	R_5	Observed pIC_{50}	Predicted pIC_{50}	Residual
1[a]	C_8H_{17}	H	H	H	$CONH_2$	0.921	1.333	0.412
2	C_8H_{17}	H	H	H	COOH	1.456	1.494	0.038
3	$OC_{10}H_{21}$	H	H	H	COOH	1.699	1.669	−0.030
4	Phenyl	H	H	H	$CONH_2$	0.823	0.788	−0.035
5	H	Phenyl	H	H	$CONH_2$	0.602	0.576	−0.026
6	Phenyl	H	H	H	COOH	1.194	1.002	−0.192
7	H	Phenyl	H	H	COOH	0.678	0.789	0.111
8[a]	4-Fluorophenyl	H	H	H	COOH	1.432	1.572	0.140
9	3-Fluorophenyl	H	H	H	COOH	1.387	1.436	0.049
10	4-Chlorphenyl	H	H	H	COOH	1.569	1.601	0.032
11	3-Chlorphenyl	H	H	H	COOH	1.721	1.583	−0.138
12	*p*-Tolyl	H	H	H	COOH	1.398	1.437	0.039
13	4-Isopropyphenyl	H	H	H	COOH	1.456	1.427	−0.029
14	4-Methoxyphenyl	H	H	H	COOH	1.046	1.219	0.173
15	Phenyl	H	F	H	COOH	0.638	0.701	0.063
16	OC_9H_{19}	H	H	H	COOH	1.638	1.633	−0.005
17	OC_8H_{17}	H	H	H	COOH	1.585	1.596	0.011
18[a]	OC_7H_{15}	H	H	H	COOH	1.495	1.566	0.071
19[a]	OC_6H_{13}	H	H	H	COOH	1.468	1.527	0.059
20	*O*-Phenyl	H	H	H	COOH	1.444	1.421	−0.023
21	O-(4-CF_3-phenyl)	H	H	H	COOH	1.721	1.637	−0.084
22	CH_2-phenyl	H	H	H	COOH	1.268	1.244	−0.024
23	$C(CH_3)_2$-phenyl	H	H	H	COOH	1.328	1.298	−0.030
24	OCH_2CH_2O-phenyl	H	H	H	COOH	0.959	0.983	0.024
25[a]	*O*-Phenyl	H	H	C(O)Me	COOH	1.921	1.772	−0.149
26	O-(4-CF_3-phenyl)	H	H	C(O)Me	COOH	2.000	2.011	0.011
27	OCH_2CH_2O-phenyl	H	H	C(O)Me	COOH	1.387	1.357	−0.030
28	*O*-Phenyl	H	H	C(O)isopropyl	COOH	1.921	2.017	0.096

[a] Test set compound

the training set molecules and the PRESS is the sum of squared deviations between predicted and observed activity values for every molecule in the test set.

HQSAR analysis for various fragment distinction combinations

For the sake of reducing the chances of bad collisions, the defaults of the HLs are set automatically by software as several prime numbers, such as 53, 59, 61, 71, 83, 97, 151, 199, 257, 307, 353, and 401. Employing these prime numbers as HLs, several combinations of these parameters were considered using the fragment size default (4–7) as follows: A/B, A/B/C, A/B/C/H, A/B/H, A/B/DA, A/B/C/DA, A/B/H/DA, and A/B/C/H/DA. The fragment distinction parameters are described as follows: A, atoms; B, bonds; C, connections; H, hydrogen atoms; DA, donor and acceptor. Due to the lack of chiral carbon atom of all the 28 molecules, the fragment distinction of chirality was not discussed in Table 2.

From what has been demonstrated in Table 2, we can obviously see that the best statistical model was derived

Table 2 HQSAR analysis for various fragment distinction combinations on the key statistical parameters using default fragment size (4–7)

Model	Fragment distinction	r^2	SEE	q^2	SEP	HL	*N*
1	A/B	0.784	0.198	0.523	0.294	307	3
2	A/B/C	0.917	0.126	0.669	0.252	257	4
3	A/B/C/H	0.917	0.126	0.663	0.254	257	4
4	A/B/H	0.762	0.208	0.503	0.300	307	3
5	A/B/DA	0.888	0.151	0.634	0.272	71	5
6	**A/B/C/DA**	**0.978**	**0.069**	**0.773**	**0.221**	**97**	**6**
7	A/B/H/DA	0.828	0.181	0.584	0.282	71	4
8	A/B/C/H/DA	0.955	0.096	0.771	0.215	53	5

The model chosen for analysis is highlighted in bold fonts

q^2 cross-validated correlation coefficient, *SEP* cross-validated standard error, r^2 non-cross-validated correlation coefficient, *SEE* non-cross-validated standard error, *HL* hologram length, *N* optimal number of components

Fragment distinction: *A* atoms, *B* bonds, *C* connections, *H* hydrogen atoms, *DA* donor and acceptor

using atoms, bonds, connections, and donor and acceptor (DA) as fragment distinction with 6 being the optimum number of PLS components showing cross-validated q^2 value of 0.773 and conventional r^2 value of 0.978. As can be seen from the comparison between model 2 and model 6, the DA played an important role in ameliorating the model quality. The important role of hydrogen bond acceptor was also reflected in the 3D-QSAR pharmacophore model (Jain *et al*., 2013). In our study, the model 6 was indicative of the possibility that the hydrogen bond donor exerted positive impact on the inhibitory activity, which is a new discovery but needs to be confirmed in further investigation. In particular, based on the model 6 in which the DA flag was enabled, the additional selection of hydrogen flag in model 8 cannot make the model better, which is ascribed to the drastic increase in the number of fragments generated when both of these options are considered (Heritage Trevor and Lowis David, 1999).

HQSAR analysis for the influence of various fragment size

Based on the best HQSAR model generated above (model 6, Table 2), the influence of different fragment sizes on statistical parameters was further investigated and summarized in Table 3. As can be seen from Table 3, the r^2 values of all models were greater than 0.94, and the q^2 values are also satisfactory. The result shown in bold fonts in Table 3 indicated that the fragment size (3–6) led to better statistical results in comparison with other fragment sizes. Therefore, the best final HQSAR model obtained

Table 3 HQSAR analysis for the influence of various fragment size using the best fragment distinction (A/B/C/DA)

Fragment size	r^2	SEE	q^2	SEP	HL	*N*
1–3	0.947	0.107	0.725	0.243	59	6
4–7	0.978	0.069	0.773	0.221	97	6
3–10	0.978	0.066	0.662	0.261	307	5
1–4	0.944	0.106	0.708	0.243	307	5
2–5	0.953	0.097	0.685	0.253	53	5
3–6	**0.961**	**0.088**	**0.790**	**0.206**	**97**	**5**
5–8	0.953	0.097	0.740	0.230	53	5
6–9	0.973	0.075	0.748	0.226	83	5
7–10	0.982	0.063	0.660	0.271	353	6
1–7	0.955	0.093	0.771	0.209	97	4

The model chosen for analysis is highlighted in bold fonts

from training set with 23 compounds was established using atoms, bonds, connections, DA as fragment distinction, and 1–7 as fragment size with 5 being the optimum number of PLS components showing cross-validated q^2 value of 0.790 and conventional r^2 value of 0.961.

The evaluation of HQSAR model quality

Since the structure encoded within a 2D fingerprint is directly related to biological activity of molecules, the HQSAR model is able to predict the activity of new related molecules according to its fingerprint. In virtue of the finally optimal QSAR model showing non-cross-validated ($r^2 = 0.961$) and cross-validated ($q^2 = 0.790$) correlation coefficients, which manifested a good internally predictive power, the predicted pIC_{50} values of both test set and training set compounds are listed in Table 1. Furthermore, the graphic results for the experimental versus predicted activities of both training set and test set are displayed in Fig. 1. The constructed HQSAR model showed good agreement between experimental and predicted values for the test set compounds with the higher predictive correlation coefficient ($r^2_{pred} = 0.605$), which signified a high external predictability of model. As far as the satisfactory performance of this holographic QSAR is considered, the model can be used to predict the biological activity of novel compounds within this structural class.

Interpretation of HQSAR contribution map

A significant role of a QSAR model is not only to predict the activities of untested molecules, but also to throw light on what molecular fragments play key roles to the contribution of biological activity. The results of the HQSAR analysis can be graphically displayed as color-coded

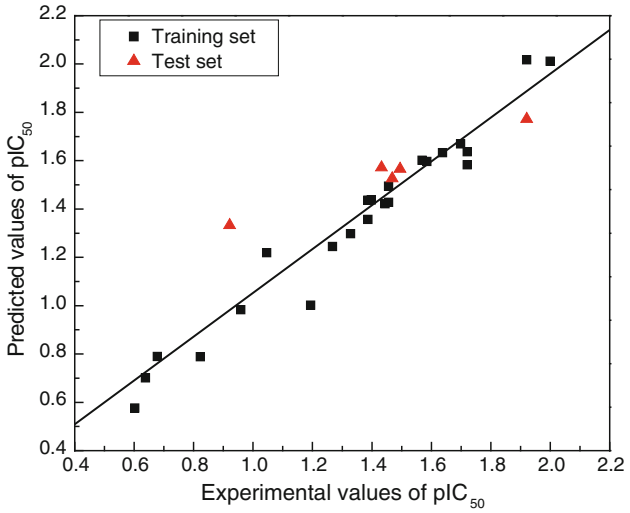

Fig. 1 Plot of experimental versus predicted pIC_{50} values of the training set and test set molecules. The training set and test set molecules are shown in *black* (*squares*) and *red* (*triangle*) *spots*, respectively

structure diagrams in which the color of each atom reflects its contribution to the molecule's overall activity. The colors at the red end of the spectrum (red and orange) represent poor contributions, while colors at the green end (yellow, blue, and green) indicate favorable contributions. HQSAR offers a good way of accounting for the variance of molecular activity by condensing information on the structural fragment.

Using the best HQSAR model, which factored atoms, bonds, connections, and DA into fragment distinction parameters, the atomic contribution maps of 23 compounds included in the training set were generated. The individual atomic contributions maps of the most (compound **26**) and least (compound **5**) potent $cPLA_2\alpha$ inhibitors, resulting from the best HQSAR model, are displayed in Fig. 2. From Fig. 2, it can be seen that the structural fragment containing the carboxylic acid moiety in 5 position of the indole ring (compound **26**) was colored yellow indicating its positive contribution to its inhibitory activity, while the amide group in the same place (compound **5**) was colored heavily red signifying its negative effect on the activity. This was a possible reason why compounds **2**, **6**, and **7** with carboxylic acid moiety on the 5 position of indole ring have higher potency than compounds **1**, **4**, and **5**. This result was consistent with previous studies, which reinforced the importance of the carboxylic acid moiety in establishing the pharmacophore of these inhibitors (Jain *et al*., 2013). In consideration of the preeminence of the carboxylic acid moiety and the newly discovered role of hydrogen bond donor in our study, we deduced that the carboxylic acid group may function as hydrogen bond donor in the interaction between the inhibitors and the active site of target

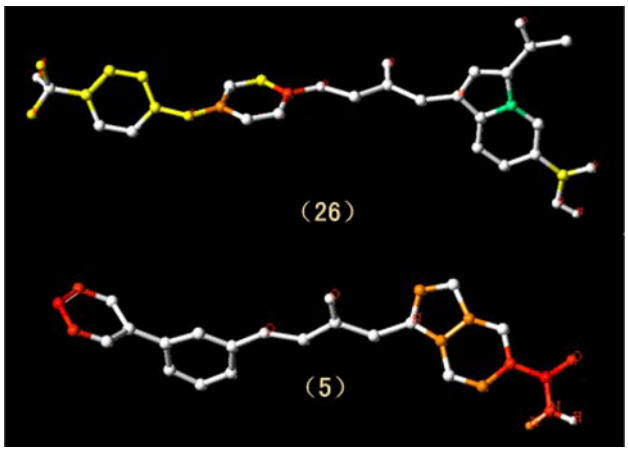

Fig. 2 Atomic contribution maps for compound **26** and compound **5**

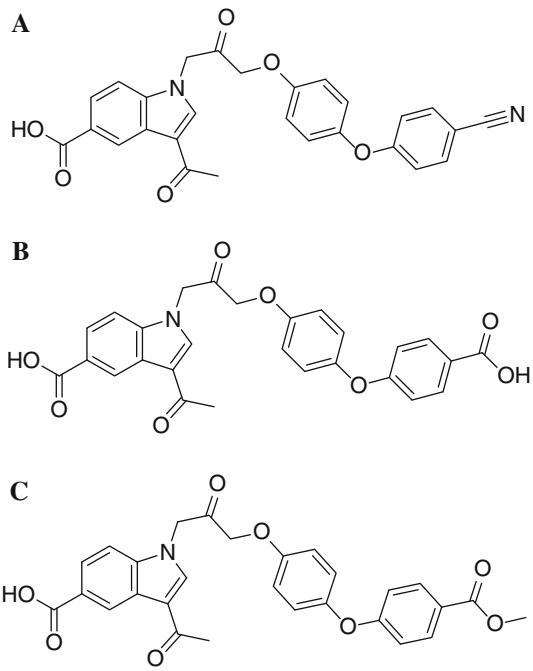

Fig. 3 Structures of new compounds and predicted pIC_{50}

enzyme, which also supported the above-mentioned hypothesis in HQSAR analysis for various fragment distinction combinations.

In particular, it is found that one fragment of the compound **26**, represented by oxygen-(4-CF_3-phenyl) moiety, was indicated to be strongly related to its biological activity. Compared with the molecular structure of compound **25** and compound **27**, the introduction of trifluoromethyl played an important role in improving the activity of compound **26**, which was probably attributed to the electron-withdrawing effect of the trifluoromethyl. The electron-withdrawing group attached to the oxygen-(4-

Table 4 Chemical structures of designed molecules and predicted activities

Compound	R_1	R_2	R_3	R_4	R_5	Predicted pIC_{50}
A	O-(4-CN-phenyl)	H	H	C(O)Me	COOH	2.011
B	O-(4-COOH-phenyl)	H	H	C(O)Me	COOH	2.094
C	O-(4-$COOCH_3$-phenyl)	H	H	C(O)Me	COOH	2.066

phenyl) may be able to strengthen inhibitory activity, which was the basis for our follow-up molecular design.

Compounds designed and activity predicted

In view of the information derived from these contribution maps, we modified the structure of compound **26** by substituting the R_4 and R_5 fragment with other groups such as propionyl and amide group, respectively. Nevertheless, the predicted activities resulting from the best HQSAR model herein established were far from satisfaction. Taking the dominant role of the carboxylic acid moiety and the electron-withdrawing effect into consideration, we further modified the structure of 1-(5-carboxyindol-1-yl)propan-2-one cPLA$_2\alpha$ inhibitors. The structures of new compounds with potentially improved biological activity are displayed in Fig. 3. In terms of the best holographic QSAR model established above, the activity of the new compounds thus designed were predicted, as shown in Table 4. From the prediction results, the biological activities (pIC_{50}) of new compounds were all greater than 2.0. These new compounds are likely to possess higher inhibitory activity but still remain to be experimentally verified.

Conclusions

In summary, we successfully generated a hologram QSAR model for 1-(5-carboxyindol-1-yl)propan-2-one cPLA$_2\alpha$ inhibitors with good statistical results. The model ($N = 5$) displayed significant cross-validated ($q^2 = 0.790$) and non-cross-validated ($r^2 = 0.961$) correlation coefficients. The high agreement between the experimental and predicted values for the test set compounds verified the reliability and robustness of the constructed HQSAR model, indicating a high external predictability of model. The importance of the structural fragment to the overall activity of this series was interpreted by the HQSAR contribution maps. Contribution maps showed that the carboxylic acid moiety in position 5 of the indole scaffold and the electron-withdrawing effects increased the inhibitory activity. Moreover, we have designed novel inhibitors of cPLA$_2\alpha$ possessing better inhibitory activity. Therefore, the HQSAR model can provide guidelines for future efforts in the design of new more active cPLA$_2\alpha$ inhibitors that are structurally related with the training set compounds.

References

Bonventre JV (2004) Cytosolic phospholipase A$_2\alpha$ reigns supreme in arthritis and bone resorption. Trends Immunol 25(3):116–119. doi:10.1016/j.it.2004.01.006

Bonventre JV, Huang Z, Taheri MR, O'Leary E, Li E, Moskowitz MA, Sapirstein A (1997) Reduced fertility and postischaemic brain injury in mice deficient in cytosolic phospholipase A2. Nature 390(6660):622–625

Chen L, Wang W, Lee KL, Shen MWH, Murphy EA, Zhang W, Xu X, Tam S, Nickerson-Nutter C, Goodwin DG, Clark JD, McKew JC (2009) Reactions of functionalized sulfonamides: application to lowering the lipophilicity of cytosolic phospholipase A2α inhibitors. J Med Chem 52(4):1156–1171. doi:10.1021/jm8009876

Clark JD, Tam S (2004) Potential therapeutic uses of phospholipase A2 inhibitors. Expert Opin Ther Pat 14(7):937–950. doi:10.1517/13543776.14.7.937

Connolly S, Robinson DH (1995) Patent update: pulmonary-allergy, dermatological, gastrointestinal and arthritis: the search for inhibitors of the phospholipases A2. Expert Opin Ther Pat 5(7):673–683. doi:10.1517/13543776.5.7.673

Cramer RD, Patterson DE, Bunce JD (1988) Comparative molecular field analysis (CoMFA). 1. Effect of shape on binding of steroids to carrier proteins. J Am Chem Soc 110(18):5959–5967. doi:10.1021/ja00226a005

Drews A, Bovens S, Roebrock K, Sunderkötter C, Reinhardt D, Schäfers M, van der Velde A, Schulze Elfringhoff A, Jr Fabian, Lehr M (2010) 1-(5-Carboxyindol-1-yl)propan-2-one inhibitors of human cytosolic phospholipase A$_2\alpha$ with reduced lipophilicity: synthesis, biological activity, metabolic stability, solubility, bioavailability, and topical in vivo activity. J Med Chem 53(14):5165–5178. doi:10.1021/jm1001088

Ghosh M, Tucker DE, Burchett SA, Leslie CC (2006) Properties of the Group IV phospholipase A2 family. Prog Lipid Res 45(6):487–510. doi:10.1016/j.plipres.2006.05.003

Hegen M, Sun L, Uozumi N, Kume K, Goad ME, Nickerson-Nutter CL, Shimizu T, Clark JD (2003) Cytosolic phospholipase A$_2\alpha$–deficient mice are resistant to collagen-induced arthritis. J Exp Med 197(10):1297–1302. doi:10.1084/jem.20030016

Heritage Trevor W, Lowis David R (1999) Molecular hologram QSAR. In: Rational drug design, vol. 719. ACS Symposium Series. American Chemical Society, pp 212–225. doi:10.1021/bk-1999-0719.ch014

Jain S, Ghate M, Bhadoriya K, Bari S, Sugandhi G, Mandwal P (2013) 3D-QSAR pharmacophore modeling and in silico screening of phospholipase A$_2\alpha$ inhibitors. Med Chem Res 22(7):3096–3108. doi:10.1007/s00044-012-0316-3

Kaptur M, Elfringhoff AS, Lehr M (2011) Structure–activity relationship studies on 1-(5-carboxyindol-1-yl)-propan-2-one inhibitors of human cytosolic phospholipase A$_2\alpha$: variation of the activated ketone moiety. Bioorg Med Chem Lett 21(6):1773–1776. doi:10.1016/j.bmcl.2011.01.085

Kita Y, Ohto T, Uozumi N, Shimizu T (2006) Biochemical properties and pathophysiological roles of cytosolic phospholipase A2s. Biochim Biophys Acta 1761(11):1317–1322. doi:10.1016/j.bbalip.2006.08.001

Klebe G, Abraham U, Mietzner T (1994) Molecular similarity indices in a comparative analysis (CoMSIA) of drug molecules to correlate and predict their biological activity. J Med Chem 37(24):4130–4146. doi:10.1021/jm00050a010

Lee KL, Foley MA, Chen L, Behnke ML, Lovering FE, Kirincich SJ, Wang W, Shim J, Tam S, Shen MWH, Khor S, Xu X, Goodwin DG, Ramarao MK, Nickerson-Nutter C, Donahue F, Ku MS, Clark JD, McKew JC (2007) Discovery of ecopladib, an indole inhibitor of cytosolic phospholipase A2α. J Med Chem 50(6):1380–1400. doi:10.1021/jm061131z

Lee KL, Behnke ML, Foley MA, Chen L, Wang W, Vargas R, Nunez J, Tam S, Mollova N, Xu X, Shen MWH, Ramarao MK, Goodwin DG, Nickerson-Nutter CL, Abraham WM, Williams C, Clark JD, McKew JC (2008) Benzenesulfonamide indole inhibitors of cytosolic phospholipase $A_2\alpha$: optimization of in vitro potency and rat pharmacokinetics for oral efficacy. Bioorg Med Chem 16(3):1345–1358. doi:10.1016/j.bmc.2007.10.060

Lehr M (2006) Inhibitors of Cytosolic Phospholipase A2 as Potential Anti-Inflammatory Drugs. Anti-Inflamm Anti-Allergy Agents Med Chem 5(2):149–161. doi:10.2174/187152306776872488

Magrioti V, Kokotos G (2010) Phospholipase A2 inhibitors as potential therapeutic agents for the treatment of inflammatory diseases. Expert Opin Ther Pat 20(1):1–18. doi:10.1517/13543770903463905

McKew JC, Lee KL, Shen MWH, Thakker P, Foley MA, Behnke ML, Hu B, Sum F-W, Tam S, Hu Y, Chen L, Kirincich SJ, Michalak R, Thomason J, Ipek M, Wu K, Wooder L, Ramarao MK, Murphy EA, Goodwin DG, Albert L, Xu X, Donahue F, Ku MS, Keith J, Nickerson-Nutter CL, Abraham WM, Williams C, Hegen M, Clark JD (2008) Indole cytosolic phospholipase A2 α inhibitors: discovery and in vitro and in vivo characterization of 4-{3-[5-chloro-2-(2-{[(3,4-dichlorobenzyl)sulfonyl]amino}ethyl)-1-(diphenylmethyl)-1H-indol-3-yl]propyl}benzoic acid efipladib. J Med Chem 51(12):3388–3413. doi:10.1021/jm701467e

Miyaura C, Inada M, Matsumoto C, Ohshiba T, Uozumi N, Shimizu T, Ito A (2003) An essential role of cytosolic phospholipase $A_2\alpha$ in prostaglandin E2—mediated bone resorption associated with inflammation. J Exp Med 197(10):1303–1310. doi:10.1084/jem.20030015

Nagase T, Uozumi N, Ishii S, Kume K, Izumi T, Ouchi Y, Shimizu T (2000) Acute lung injury by sepsis and acid aspiration: a key role for cytosolic phospholipase A2. Nat Immunol 1(1):42–46

Sapirstein A, Bonventre JV (2000) Specific physiological roles of cytosolic phospholipase A2 as defined by gene knockouts. Biochim Biophys Acta 1488(1–2):139–148. doi:10.1016/S1388-1981(00)00116-5

Seno K, Okuno T, Nishi K, Murakami Y, Watanabe F, Matsuura T, Wada M, Fujii Y, Yamada M, Ogawa T, Okada T, Hashizume H, Kii M, Hara S, Hagishita S, Nakamoto S, Yamada K, Chikazawa Y, Ueno M, Teshirogi I, Ono T, Ohtani M (2000) Pyrrolidine inhibitors of human cytosolic phospholipase A(2). J Med Chem 43(6):1041–1044

Seno K, Okuno T, Nishi K, Murakami Y, Yamada K, Nakamoto S, Ono T (2001) Pyrrolidine inhibitors of human cytosolic phospholipase A2. Part 2: synthesis of potent and crystallized 4-triphenylmethylthio derivative 'Pyrrophenone'. Bioorg Med Chem Lett 11(4):587–590. doi:10.1016/S0960-894X(01)00003-8

Uozumi N, Kume K, Nagase T, Nakatani N, Ishii S, Tashiro F, Komagata Y, Maki K, Ikuta K, Ouchi Y, J-i Miyazaki, Shimizu T (1997) Role of cytosolic phospholipase A2 in allergic response and parturition. Nature 390(6660):618–622